

Temperature Dependence of Penetration Depth and Surface Resistance of $\text{Nd}_{1.85}\text{Ce}_{0.15}\text{CuO}_4$

Dong Ho Wu, Jian Mao, S. N. Mao, J. L. Peng, X. X. Xi, T. Venkatesan, R. L. Greene,
and Steven M. Anlage

Center for Superconductivity Research, Department of Physics, University of Maryland, College Park, Maryland 20742
(Received 25 September 1992)

The temperature dependence of the in-plane penetration depth λ_{\parallel} and surface resistance R_s at 9.6 GHz were measured for high-quality $\text{Nd}_{1.85}\text{Ce}_{0.15}\text{CuO}_4$ thin films and single crystals. Both $\lambda_{\parallel}(T)$ and $R_s(T)$ are well described within the BCS framework over the entire temperature range below T_c , yielding an energy gap ratio $2\Delta/k_B T_c = 4.1 \pm 0.2$ and the London penetration depth $\lambda_{L\parallel}(0) \sim 1000 \text{ \AA}$. These results indicate that the electrodynamics of this *n*-type cuprate superconductor are consistent with a single-gap *s*-wave BCS behavior.

PACS numbers: 74.30.Gn, 74.20.-z, 74.70.-b, 74.75.+t

The pairing mechanism responsible for superconductivity in the high- T_c copper oxide materials is still unknown. Experiments to address this fundamental question have been focused on the hole-doped superconductors, in particular, $\text{YBa}_2\text{Cu}_3\text{O}_7$ (YBCO) and $\text{Bi}_2\text{Sr}_2\text{CaCu}_2\text{O}_8$ (BSCCO), where high-quality single crystals and thin films are available. Studies of the electrodynamic properties provide a clear phenomenological picture, reveal information regarding the pairing state, energy gap, and density of states of the superconductor, and give important insights into the mechanisms of high- T_c superconductivity. However, there is no clear consensus about the electrodynamics of the cuprates from earlier studies of YBCO and BSCCO [1]. This is due, in part, to their complex microstructural properties: interruption of the conductive Cu-O chains by twin boundaries in YBCO, and the short coherence length [for example, in-plane coherence length $\xi_{\parallel}(0) \sim 10\text{--}15 \text{ \AA}$] which gives rise to a plethora of weak-link phenomena [2]. In the electron-doped $\text{Nd}_{1.85}\text{Ce}_{0.15}\text{CuO}_4$ (NCCO), there are no Cu-O chains, and the coherence length is considerably longer [$\xi_{\parallel}(0) \sim 80 \text{ \AA}$] than in the other cuprates, making this material more suitable for studying the intrinsic electrodynamics of the cuprates.

Little progress has been made with NCCO up to this time because of the difficulties [3] in preparing homogeneous, single-phase samples. As part of this work, we have examined over twenty samples and found that the electrodynamic properties of NCCO are sample dependent: For high-quality samples a single sharp transition and reproducible results are typical, while for poor samples multiple transitions and irreproducible results are common, particularly at high frequencies. Information obtained from our microwave measurements and other types of characterization [4] have been used to improve the sample quality. With this iterative trial-and-error method, we have dramatically improved the quality of both thin films and single crystals of NCCO [4]. In this Letter we report, for the first time, experimental results on the temperature-dependent in-plane penetration depth $\lambda_{\parallel}(T)$ and surface resistance $R_s(T)$ of high-quality NCCO samples, measured at 9.6 GHz. In addition, we

report a comparison of $\lambda_{\parallel}(T)$ at 9.6 GHz and at zero frequency, measured using a dc SQUID at low fields ($\leq 0.3 \text{ Oe}$). The results from the high-quality samples clearly show that electrodynamic behavior of the material is very similar to that of conventional superconductors. The temperature dependences of λ_{\parallel} and R_s are consistent with a BCS calculation with gap ratio $2\Delta(0)/kT_c \approx 4.1$ and London penetration depth $\lambda_{L\parallel} \approx 1000 \text{ \AA}$ for currents flowing in the copper-oxygen plane.

Details of the fabrication and sample characterization of the high-quality *c*-axis-oriented thin films on LaAlO_3 substrates, and single crystals, are discussed elsewhere [4]. The typical sizes for thin films and single crystals are $2.6 \times 5.6 \text{ mm}^2$ with a thickness $\sim 5000 \text{ \AA}$ and $2 \times 2 \text{ mm}^2$ with a thickness $\sim 20 \text{ \mu m}$, respectively. Both thin films and single crystals show a single sharp transition ($\leq 0.2 \text{ K}$ wide in an ac susceptibility or in a dc SQUID characterization) at $T_c \sim 21\text{--}22 \text{ K}$, and other characterization such as x-ray diffraction verified the samples were single phase.

Measurements of the complex surface impedance $Z_s (=R_s + i\omega\mu_0\lambda)$ at 9.6 GHz were carried out by employing a superconducting Nb cavity [5] with the sample on a hot finger. The superconducting Nb cavity was thermally treated to obtain recrystallized surfaces, rendering a very high Q ($\geq 2.2 \times 10^7$) and stable resonant frequency ($\delta f/f < 2 \times 10^{-9}$) at the cavity temperature $T \leq 4.2 \text{ K}$. Changes in Q and the resonant frequency f of the cavity are related to R_s and changes $\delta\lambda$ by $R_s = \Gamma(1/Q - 1/Q_{\text{cav}})$ and $\delta\lambda = -\zeta\delta f$, where Γ and ζ are geometric factors and Q_{cav} is the Q of the cavity with the sample absent. The geometrical factors were carefully determined experimentally by using Nb samples of dimensions similar to the $\text{Nd}_{1.85}\text{Ce}_{0.15}\text{CuO}_4$ samples. In this work, the background temperature dependence is negligible and does not limit the resolution for either R_s or λ . With a typical size of thin film, we achieved a resolution $R_s \sim 10 \text{ \mu}\Omega$ and $\delta\lambda \lesssim 3 \text{ \AA}$, over the entire temperature range.

In Fig. 1 we show typical results for $1/Q(T)$ and $\delta f(T)$ for $T/T_c \leq 0.5$, for a thin film. The insets are for the entire temperature range. Bearing the relations $\delta\lambda \propto \delta f$ and $R_s \propto 1/Q$ in mind, we can discern the tempera-

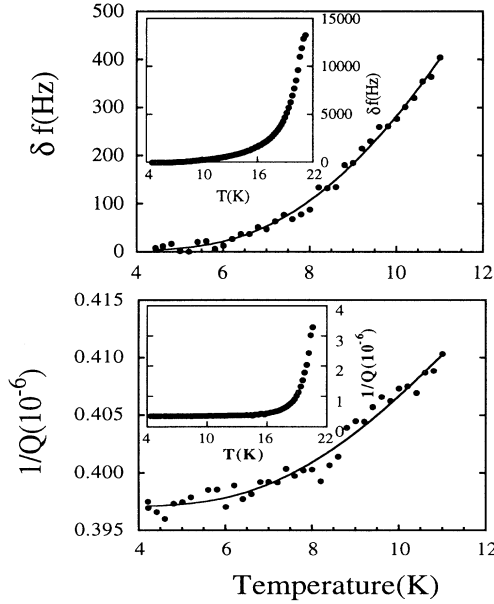


FIG. 1. Temperature dependence of δf and $1/Q$ for $T/T_c < 0.5$ for a NCCO thin film. The solid lines are the best fit to data which show $\delta f(T) \propto (1/\sqrt{T})\exp[-\Delta(0)/k_B T]$ and $1/Q \propto (1/T)\exp[-\Delta(0)/k_B T]$, both with $2\Delta(0)/k_B T_c = 4.1$. Insets: δf and $1/Q$ for entire temperature range.

ture dependence of $\delta\lambda$ and R_s directly from the raw data, particularly at low temperatures since it is widely believed that the symmetry of the pairing state [6] of a superconductor is directly manifested in the low-temperature dependence of Z_s . The best fit of $\delta f(T)$ can be obtained with an exponential dependence [7] $\delta f(T) \propto (1/\sqrt{T})\exp[-\Delta(0)/k_B T]$ with $\Delta(0)/k_B = 43$ K [implying the energy gap ratio $2\Delta(0)/k_B T_c \approx 4.1$]. Other functional forms such as T^2 and $1/[1 - (T/T_c)^2]^{1/2}$ dependences, which have been reported [8] in YBCO, are not reconcilable with our data for $\delta f(T)$. In the fit for $1/Q(T)$, identical results were obtained, i.e., the exponential dependence [8] $1/Q(T) \propto (1/T)\exp[-\Delta(0)/k_B T]$ and the gap ratio $2\Delta(0)/k_B T_c = 4.1$. Hence, both the Q and f data strongly suggest the s -wave BCS-type temperature dependence of R_s and $\lambda_{||}$ at low temperatures.

In our data, the BCS-like features are not limited to low temperatures but also continue up to near T_c [9], and, moreover, the data show a clear quantitative agreement with the BCS description. In Fig. 2, a comparison with a detailed BCS calculation, with the frequency- and wave-vector-dependent kernel [7], is made for two typical data sets of $\lambda_{||}(T)$: one from a thin film at 9.6 GHz and the other from a single crystal at zero frequency using a method similar to Ref. [10]. Both of them exhibit the s -wave BCS-like temperature dependence in general, although the latter is less obvious because of a much larger experimental error (the sensitivity of the dc SQUID is $\delta M/M \lesssim 10^{-3}$). The numerical calculation requires several parameters, including a measurement frequency f , transition temperature T_c , the London penetration depth

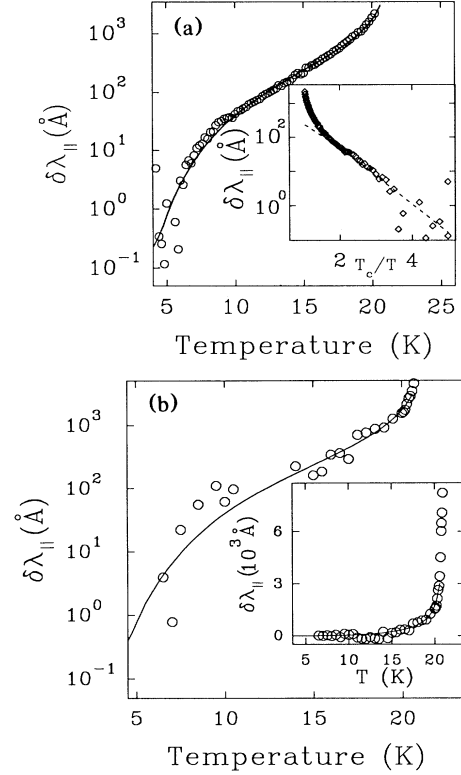


FIG. 2. (a) Change in penetration depth $\delta\lambda_{||}(T)$ at 9.6 GHz for a NCCO thin film. The solid line represents the BCS calculation with $2\Delta(0)/k_B T_c = 4.1$. Inset: $\delta\lambda_{||}$ vs T_c/T . Note the exponential behavior (dashed line) $\delta\lambda_{||}(T) = \lambda(0)[\frac{1}{2}\pi\Delta(0)/k_B T]^{1/2} \times \exp[-\Delta(0)/k_B T]$ for $T_c/T \geq 2$. (b) $\delta\lambda_{||}(T)$ extracted from a dc magnetization measurement for a $\text{Nd}_{1.85}\text{Ce}_{0.15}\text{CuO}_4$ single crystal with a BCS fit for $2\Delta(0)/k_B T_c = 4.2$. Inset: Linear plot of $\delta\lambda_{||}(T)$.

$\lambda_L(0)$, the coherence length ξ , the mean free path l , and $\Delta(0)/k_B T_c$. The typical parameter values for the best fit are listed in Table I. Frequency dependence of the parameters is not seen in this work, and is possibly less than the error ($\sim 10\%$) in determining the parameter values.

The in-plane coherence length $\xi_{||}(0) \approx 80$ Å (this agrees with Ref. [11]) was estimated from the relation $\xi_{||}(\Phi_0/2\pi H_{c2\perp})^{1/2}$ while $H_{c2\perp}(T)$ and then $H_{c2\perp}(0) = -0.69T_c(dH_{c2\perp}/dT)_{T=T_c}$ were extracted from magneto-resistance measurements which were carried out in addition to the microwave measurements. An estimate of the mean free path $l \sim 115$ – 230 Å is obtained from an experiment and analysis similar to Ref. [12]. However, because considerable uncertainty is involved in determining l , we have further adjusted the value of l in the BCS calculations. The temperature dependence of l in the superconducting state is not known, and was assumed to be constant in this analysis.

Although l , λ_L , and $\Delta(0)/k_B T_c$ are used as free parameters, we adjust the values within certain ranges, because the experimentally determined effective penetration depth λ^{eff} constrains λ_L through $\lambda^{\text{eff}} = \lambda_L [1 + \xi_0/J(R=0, T)]^{1/2}$

TABLE I. Electrodynamic parameters used to fit the $\lambda_{\parallel}(T)$ and $R_s(T)$ data with the BCS calculation for $\text{Nd}_{1.85}\text{Ce}_{0.15}\text{CuO}_4$. Parameters above the center line were determined by independent means, and those below the line were used as fitting parameters.

| | Microwave measurements | | dc magnetization |
|-------------------------------|------------------------|-----------------|------------------|
| | Thin films | Single crystals | Single crystals |
| T_c (K) | 21 | 21.5 | 22 |
| $\lambda_{\parallel}(0)$ (Å) | 1300 ± 100 | 1250 ± 200 | 1100 ± 300 |
| $\xi_{\parallel}(0)$ (Å) | 72–80 ^a | 80 | N/A |
| R_0 (mΩ) | 2.5 | 1 | N/A |
| l (Å) | 115–600 ^a | 300 ± 200 | N/A |
| $2\Delta/kT_c$ | 4–4.3 | 3.9–4.3 | 3.9–4.5 |
| $\lambda_{L\parallel}(0)$ (Å) | 1000 ± 90 | 1050 ± 200 | N/A |

^aFor $R_s(T)$, $\xi_{\parallel}(0) \sim 72$ Å and $l \sim 600$ Å. For $\lambda_{\parallel}(T)$, $\xi_{\parallel}(0) \sim 80$ Å and $l \sim 100$ Å.

where $J(0, T)$ is the BCS range function with a value $1 \leq J(0, T) \leq 1.33$. Further, the interplay between λ_L and $\Delta(0)/k_B T_c$ could change the value of λ_L as $\Delta(0)/k_B T_c$ varies. Considering these, we plot $d\lambda_{\parallel}/dy$ vs $y \equiv 1/[1-t^4]^{1/2}$, as shown in Fig. 3, which shows the value of $d\lambda_{\parallel}/dy$ at $y > 2$ converges to yield $\lambda_{\parallel}^{\text{eff}}(0) \sim 1300 \pm 100$ Å. Using the value $\xi_0 \sim 80$ Å and $l \sim 115$ Å, we deduce $\lambda_{L\parallel} \sim 1000 \pm 90$ Å. We found that these values, along with a choice of gap ratio $\Delta(0)/k_B T_c = 4.1 \pm 0.2$, yield the best fit (solid lines in Fig. 2 and Fig. 3) for our experimental $\lambda_{\parallel}(T)$ data.

We also note that in Fig. 3, $d\lambda_{\parallel}/dy$ diverges at $y < 1.3$, similar to what Schawlow and Devlin and other investigators [13] had seen in conventional superconductors as evidence of a finite-energy-gap behavior. Indeed, in Fig. 3, we show *without any ambiguity the BCS features* with the gap ratio $2\Delta/k_B T_c = 4.06$ [corresponding to $\Delta(0) \sim 3.67$ meV]. This value of the energy gap is in good agreement with tunneling results on a NCCO crystal by Huang *et al.* [14], and is also consistent with the gap value obtained from the exponential dependence of the

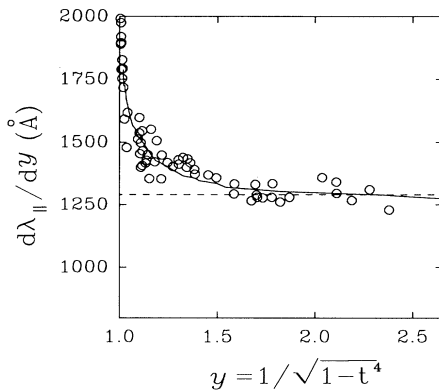


FIG. 3. $d\lambda_{\parallel}/dy$ as a function of $y = 1/(1-t^4)^{1/2}$ for a NCCO thin film. The solid line is a BCS calculation. The horizontal dashed line is a two-fluid temperature dependence with $\lambda_{\parallel}(T) = (1300 \text{ Å})/[1 - (T/T_c)^4]^{1/2}$ and $T_c = 21$ K.

raw $f(T)$ and $Q(T)$ data. Using $\lambda(0) \approx 1000$ Å, $\Delta(0)/k_B T_c = 2.03$, and the BCS expression in the low-temperature limit,

$$\lambda(T) - \lambda(0) = \lambda(0) \left[\frac{1}{2} \pi \Delta(0)/k_B T \right]^{1/2} \exp[-\Delta(0)/k_B T],$$

we obtained an excellent quantitative description for $\delta\lambda_{\parallel}(T)$ at low temperatures (dashed line in Fig. 2). This detailed agreement for $\lambda_{\parallel}(T)$ implies a *single-gap s-wave* BCS-like behavior over the entire temperature range, in strong contrast to $\lambda_{\parallel}(T)$ and $R_s(T)$ measurements in YBCO [15].

These electrodynamic properties are further validated by the results of R_s measurements, in which we cross examine several fundamental properties which were identified from $\lambda_{\parallel}(T)$. The behavior of $R_s(T)$ for a thin film is shown in Fig. 4. To obtain a quantitative agreement (solid line) between the theoretical R_s and the experimental R_s^{expt} , we use parameter values which are modified slightly from those for $\lambda_{\parallel}(T)$, and further use a modified relation $A^* R_s = R_s^{\text{expt}} - R_0$ where A^* is a correction factor, and R_0 the temperature-independent residual resistance, as is commonly done with conventional superconductors [7,9]. The correction factor $A^* \sim 1.35$ used in this work implies that the parameter values are reasonable. Nevertheless, what is significant is *the remarkable agreement over orders of magnitude between R_s^{expt} and the BCS calculation in the entire temperature range*, as well as the clear exponential behavior $R_s \propto [(\hbar\omega)^2/kT] \ln(4kT/\hbar\omega) \exp(-\Delta/kT)$ at low temperatures.

Since λ and R_s are magnetic-field dependent, and the comparison with the BCS calculation is valid only in the Meissner state, we need to prove that our results represent those of the Meissner state. Figure 5 shows a typical microwave field dependence of R_s with a thin-film sample, at $T = 20.7$ K. The data can be represented as $\delta R_s(H_{\text{rf}}) \equiv R_s(H_{\text{rf}}, T) - R_s(0, T) = g(T) H_{\text{rf}}^2$, where $R_s(0, T)$ is the surface resistance at zero field, $g(T)$ is an ex-

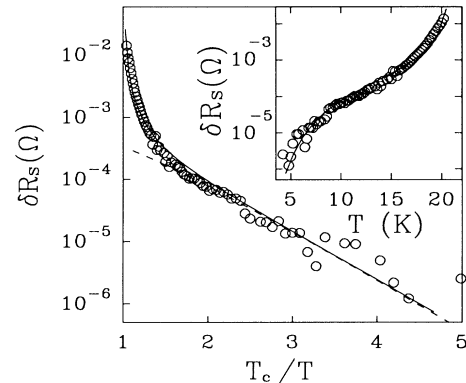


FIG. 4. δR_s vs T_c/T for a NCCO thin film at 9.6 GHz with a BCS calculation (solid line). Exponential behavior (dashed line) of $\delta R_s(T) \propto [(\hbar\omega)^2/k_B T] \ln(4k_B T/\hbar\omega) \exp(-\Delta/k_B T)$ at low temperatures ($T_c/T > 2$) with $2\Delta/k_B T_c = 4.1$. Inset: δR_s vs T .

perimentally determined coefficient, and H_{rf} is the rf magnetic-field strength parallel to the sample surface. This quadratic effect is a typical signature [16] that the sample is in the Meissner state where $H_{rf} < H_{c1}$. Because the microwave power used for measuring $\lambda(T)$ and $R_s(T)$ is in the range of $-17 \text{ dBm} < P_{\mu\text{-wave}} < 5 \text{ dBm}$ (i.e., $H_{rf} < 3 \text{ Oe} < H_{c1}$) throughout the entire experiment, we believe our experimental results for $\lambda(T)$ and $R_s(T)$ represent those of the Meissner state.

We next explore the relationship of our experimental results with other physical parameters measured by other techniques. From the Ginzburg-Landau model [17] (expected to hold near T_c), we derive the quadratic coefficient $g(T) = [R_s(0)/2H_c^2]\Delta(0)/kT$ to first-order approximation for $H_{rf} < H_{c1}$. Using the measured values $g(20.7 \text{ K}) = 2.4 \times 10^{-5} \text{ } \Omega/\text{Oe}^2$, and $R_s(0) = 18 \times 10^{-3} \text{ } \Omega$ at $T = 20.7 \text{ K}$, and the relation $H_c = H_{c0}[1 - (T/T_c)^2]$, we estimate the zero-temperature thermodynamic critical field $H_{c0} \approx 2 \text{ kOe}$. This value is larger than that of polycrystalline $\text{Sm}_{1.85}\text{Ce}_{0.15}\text{CuO}_4$ [18] ($\sim 431 \text{ Oe}$), but comparable to the estimated $H_c(0) \approx 2.5 \text{ kOe}$, obtained from $H_c = \Phi_0/2\sqrt{2}\pi\xi\lambda_L$ using $\xi = 80 \text{ } \text{Å}$ and $\lambda_L = 1000 \text{ } \text{Å}$. Also using the in-plane effective penetration depth $\lambda_{\parallel} \sim 1300 \text{ } \text{Å}$, the lower critical field $H_{c1\perp}(0) = 320 \text{ Oe}$ can be estimated from $H_{c1\perp} = (\Phi_0/4\pi\lambda_{\parallel}^2)[\ln(\lambda_{\parallel}/\xi_{\parallel}) + 0.5]$. This value is an order of magnitude larger than a published value for a polycrystalline $\text{Sm}_{1.85}\text{Ce}_{0.15}\text{CuO}_{4-y}$ [18] and comparable to $H_{c1\perp}$ of $\text{YBa}_2\text{Cu}_3\text{O}_7$ [19].

We believe that NCCO may be the simplest and most easily understood example of cuprate superconductivity because of its low T_c and relatively isolated CuO_2 planes. Previous work on the fundamental physics of the cuprates has concentrated on the high- T_c hole-doped Y, Bi, and Tl families, where a number of problems occur, as discussed earlier. With the observation of s -wave BCS-like behavior in NCCO, some questions naturally arise: Why do electrodynamic measurements on the other cuprates display non-BCS behavior [15]? Is this due to extrinsic phenomena, or a consequence of different pairing state symmetries in the other cuprates and in NCCO? These questions call for further systematic and detailed studies of the electrodynamic properties of all the cuprates.

In summary, we have shown that the experimental $\lambda_{\parallel}(T)$ and $R_s(T)$ of NCCO display clear quantitative agreement with the s -wave BCS theory, and other electrodynamic parameters interrelated to λ_{\parallel} and R_s also are entirely self-consistent. This indicates, in contrast to other high-temperature superconductors and theoretical suggestions for high-temperature superconductivity, NCCO has a single-valued and finite gap ratio throughout the entire temperature range below T_c , and its electrodynamic properties are well explained within the conventional theory. Thus the nature of the superconducting state of the n -type high-temperature superconductor is possibly very similar to that of conventional superconductors, supporting some earlier speculation [11,14] for such similari-

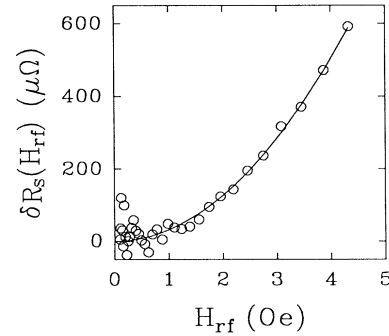


FIG. 5. Microwave field dependence of $\delta R_s(H_{rf})$ for a NCCO thin film at $T = 20.7 \text{ K}$. Solid line represents $\delta R_s(H_{rf}) = g(T)H_{rf}^2$ with $g(20.7 \text{ K}) = 24 \text{ } \mu\Omega/\text{Oe}^2$.

ty between NCCO and conventional superconductors.

We thank S. Sridhar and C. Lobb for useful discussions, and P. Kneisel for Nb cavity recrystallization. This work was supported by NSF Grant No. DMR-9115384, and an NSF NYI grant (S.M.A.).

- [1] H. Peil and G. Müller, IEEE Trans. Mag. **27**, 854 (1991).
- [2] J. Halbritter, J. Appl. Phys. **68**, 6315 (1990).
- [3] R. Lightfoot *et al.*, Physica (Amsterdam) **168C**, 627 (1990); A. R. Drews *et al.*, Physica (Amsterdam) **200C**, 122 (1992).
- [4] S. N. Mao *et al.*, Appl. Phys. Lett. **61**, 2356 (1992); J. L. Peng *et al.* (to be published).
- [5] S. Sridhar and W. Kennedy, Rev. Sci. Instrum. **59**, 531 (1988).
- [6] J. F. Annett, N. Goldenfeld, and S. R. Renn, Phys. Rev. **B 43**, 2778 (1991).
- [7] J. P. Turneaure, J. Halbritter, and H. A. Schwettman, J. Supercond. **4**, 341 (1991).
- [8] J. M. Pond *et al.*, Appl. Phys. Lett. **59**, 3033 (1991).
- [9] Very near T_c , both measured $\lambda_{\text{meas}}(T)$ and $R_s^{\text{meas}}(T)$ were corrected using $\lambda_{\text{meas}} = \lambda_{\text{true}} \tanh(d/\lambda_{\text{true}})$ and $R_s^{\text{meas}} = R_s^{\text{true}} \tanh(d/\lambda_{\text{true}})$ for the size effect due to the finite film thickness d .
- [10] L. Krusin-Elbaum *et al.*, Phys. Rev. Lett. **62**, 217 (1989).
- [11] Yoshikazu and M. Suzuki, Nature (London) **338**, 635 (1989).
- [12] S. J. Hagen *et al.*, Phys. Rev. **B 45**, 515 (1992).
- [13] A. L. Schawlow and G. E. Devlin, Phys. Rev. **113**, 120 (1959); P. C. L. Tai, M. R. Beasley, and M. Tinkham, Phys. Rev. **B 11**, 411 (1975).
- [14] Q. Huang *et al.*, Nature (London) **347**, 369 (1990).
- [15] S. M. Anlage *et al.*, Phys. Rev. **B 44**, 9764 (1991); N. Klein, J. Supercond. **5**, 195 (1992).
- [16] S. Sridhar, Dong Ho Wu, and W. Kennedy, Phys. Rev. Lett. **63**, 1873 (1989).
- [17] V. L. Ginzburg and L. D. Landau, Zh. Eksp. Teor. Fiz. **20**, 1969 (1950).
- [18] C. C. Almasan *et al.*, Phys. Rev. **B 45**, 1056 (1992).
- [19] Dong Ho Wu and S. Sridhar, Phys. Rev. Lett. **65**, 2074 (1990).